[4]Jiang, G. S., and Shu, C. W., "Efficient Implementation of Weighted ENO Schemes," *Journal of Computational Physics*, Vol. 126, No. 1, 1996, pp. 202–228.

[5]Sommerfeld, M., and Müller, H. M., "Experimental and Numerical Studies of Shock Wave Focusing in Water," *Experiments in Fluids,* Vol. 6, No. 3, 1998, pp. 209–216.

[6]Olivier, H., and Grönig, H., "The Random Choice Method Applied to Two-Dimensional Shock Focusing and Diffraction," *Journal of Computational Physics*, Vol. 63, No. 1, 1986, pp. 85–106.

[7]Isuzugawa, K., and Horiuchi, M., "Experimental and Numerical Studies of Blast Wave Focusing in Water," *Proceedings of the 18th International Symposium on Shock Waves*, Vol. 1, Springer–Verlag, New York, 1992, pp. 347–350.

[8]Shu, C. W., Zang, T. A., Erlebacher, G., Whitaker, D., and Osher, S., "High-Order ENO Schemes Applied to Two- and Three-Dimensional Compressible Flow," *Applied Numerical Mathematics*, Vol. 9, No. 1, 1992, pp. 45–71.

[9]Liu, X. D., Osher, S., and Chan, T., "Weighted Essentially Non-Oscillatory Schemes," *Journal of Computational Physics*, Vol. 115, No. 1, 1994, pp. 200–212.

[10]Thompson, W., "Time Dependent Boundary Conditions for Hyperbolic Systems," *Journal of Computational Physics*, Vol. 68, No. 1, 1987, pp. 1–24.

[11]Liang, S.-M., Tsai, C.-J., and Wu, L.-N., "Efficient, Robust Second-Order Total Variation Diminishing Scheme," *AIAA Journal,* Vol. 34, No. 1, 1996, pp. 193–195.

M. Sichel
Associate Editor

Diode-Laser Sensor for Velocity Measurements in Hypervelocity Flows

S. D. Wehe,* D. S. Baer,† and R. K. Hanson‡
Stanford University, Stanford, California 94305-3032

Introduction

REFLECTED shock tunnels have been used to provide high-enthalpy hypersonic flowfields for ground-testing applications for about 40 years.[1] High-velocity flow in these tunnels is generated from the conversion of the enthalpy in the tunnel reservoir to directed motion (kinetic energy) of the gas through a steady expansion process via a nozzle. The freestream conditions for the expanded flow are typically calculated from nonequilibrium multidimensional nozzle codes,[2,3] generally based on input from side-wall pressure and shock-speed measurements near the shock tube end wall. Experimental determinations of the freestream conditions and the steady-state test time have been very limited and generally indirect, and there have apparently been no previous diagnostics capable of time-resolved velocity measurements. This Note describes the development and implementation of a compact sensor, based on absorption spectroscopy techniques and comprising tunable diode lasers and fiber optics, that capitalizes on the natural presence of chemically frozen atomic potassium (K) for the direct determination of gas velocity from measurements of Doppler-shifted absorption line shapes. The large line strength of the probed potassium transition ($^2S_{1/2} \rightarrow {}^2P_{1/2}$) near 770 nm allows the determination of velocity from absorption measurements of trace concentrations (either naturally present or intentionally seeded) over path lengths of a few centimeters. The compact sensor (containing the optoelectronics for direct absorption measurements) was inserted into the flowfield to provide velocity measurements with relatively high spatial resolution.

Received 29 January 1999; revision received 12 April 1999; accepted for publication 21 April 1999. Published by the American Institute of Aeronautics and Astronautics, Inc., with permission.

*Research Assistant, High Temperature Gasdynamics Laboratory, Department of Mechanical Engineering.

†Research Associate, High Temperature Gasdynamics Laboratory, Department of Mechanical Engineering.

‡Professor, High Temperature Gasdynamics Laboratory, Department of Mechanical Engineering.

Diagnostic Description

The diode laser sensor was applied to measure velocity in the Calspan 96-in. hypersonic shock tunnel. The operational details and capabilities of the facility have been published previously.[4] The design of this second-generation sensor is conceptually similar to that of a larger probe developed previously for simultaneous near-infrared (1.3–1.4 μm) H_2O absorption measurements of temperature, species concentration, and velocity in hypersonic flows.[5,6] Figure 1 shows the layout of the optoelectronics within the probe. The probe was installed directly into the flowfield, 25 cm below the nozzle centerline, to minimize complications due to boundary layers and facility vibration. The nozzle exit diameter is 121 cm. The probe walls were constructed with 1.6-mm thick stainless steel for structural integrity. No cooling was required due to the short flow times.

The wavelength of the (AlGaAs) diode laser was current tuned at a 10-kHz repetition rate over the potassium D_1 ($^2S_{1/2} \rightarrow {}^2P_{1/2}$) transitions near 770 nm to record a Doppler-shifted absorption feature every 0.1 ms. The laser linewidth ($\Delta\nu_{\text{laser}} = 150 \pm 10$ MHz) was measured with a high finesse ($F = 50$ and free spectral range = 2 GHz at 770 nm) confocal Fabry–Perot interferometer. The optical output (nominal power = 9mW) of the laser was split (60:40) by a cube beam splitter (with a near-infrared antireflection coating) into two beams. The higher intensity beam was coupled into a single-mode (4.5-μm core diameter) fiber and directed 30 m through a hardened conduit to the probe. The lower intensity beam was directed through the confocal interferometer. The transmission through the interferometer was recorded with a silicon photodetector (10-MHz bandwidth) and was used to convert the signal from the time domain to the laser frequency domain. All of the voltage signals were acquired at a sampling rate of 5 MHz (0.2 μs/point) with 12-bit resolution.

Inside the probe, the laser light was divided by a cube beam splitter into two beams that were directed from one probe finger to the other at a 43.8-deg angle (Doppler-shifted beam) and a 90-deg angle (non-Doppler-shifted beam) with respect to the bulk gas velocity. Wedged (1 deg) windows were mounted in the probe to minimize etalon effects. The laser transmission intensities (~0.3 mW/mm^2) were monitored with silicon photodetectors (2.3-MHz bandwidth) inside the probe. A number 29 Wratten filter (long-pass cutoff wavelength = 630 nm) was affixed to the inside of the upper window, that is, on the receiving finger of the probe in Fig. 1, served to exclude detection of background emission.

Gas velocity was determined from the measured absorption line shapes using the Doppler relation, which relates the measured spectral shift $\Delta\nu$ (in gigahertz), at laser frequency ν, to the gas velocity V_{gas} (in meters per second):

$$\Delta\nu/\nu = V_{\text{gas}}(\cos\theta/c) \tag{1}$$

where c is the speed of light in meters per second and θ is the angle between the beam and the bulk gas velocity. The absorption measurement recorded in situ over a path perpendicular to the bulk-flow direction affords a simple means of nulling the possible effect of pressure shift in the recorded line shapes.

The theoretical basis for determining species concentration from measured absorption spectra is well established.[7,8] The K concentration was determined from the application of Beer's law:

$$-\int_{-\infty}^{\infty} \ell n\left(\frac{I_\nu}{I_\nu^0}\right) \mathrm{d}\nu = SP_iL \tag{2}$$

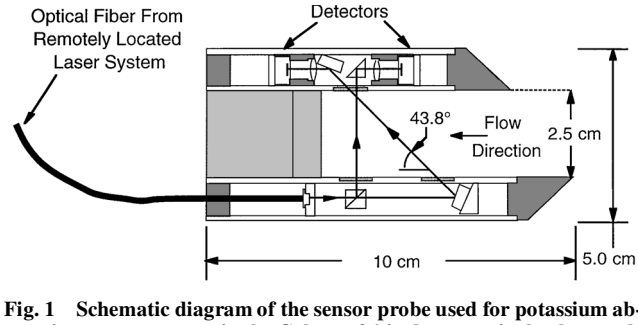

Fig. 1 Schematic diagram of the sensor probe used for potassium absorption measurements in the Calspan 96-in. hypersonic shock tunnel.

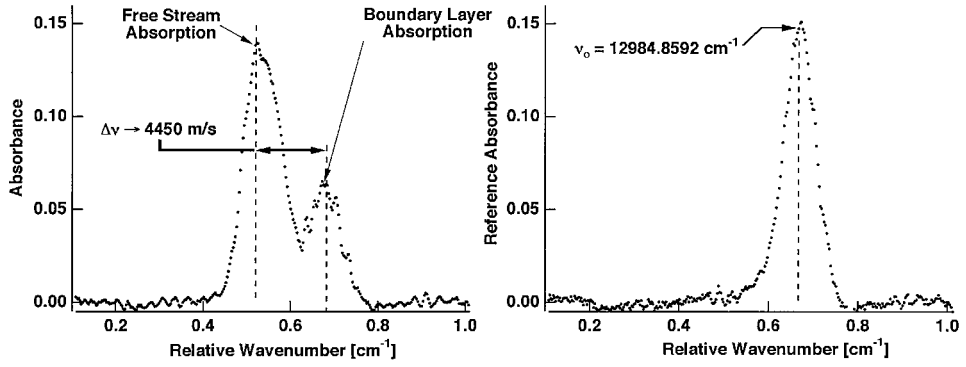

Fig. 2 Single-sweep potassium absorption line shapes ($\lambda_0 = 770.108$ nm) obtained during a 9.53-MJ/kg test. The left-hand trace was obtained from a beam directed at a 43.8-deg angle with respect to the bulk gas flow. The right-hand trace was obtained from a beam directed at a 90.0-deg angle with respect to the bulk gas flow.

where I_ν and are I_ν^0 the measured transmitted and incident intensities, respectively, S is the line strength (per square centimeter per atmosphere) of the probed transition, P_i is the partial pressure (atm) of the absorbing species, L is the known path length (centimeter), and the quantity SP_iL is the absorbance. For the temperature range of current interest, the line strength at the test condition temperature $S(T)$ may be expressed as

$$S(T) \cong S_0(T_0/T) \tag{3}$$

where $T_0 = 296$ K and S_0 is the line strength (at T_0) $= 7.28 \times 10^6$ cm^{-2} atm^{-1} (Ref. 9). Calculated values of freestream pressure and temperature for the steady-state test condition were 3 torr and 485 K in the experiment reported here.

It is assumed that potassium is present in natural isotopic proportions (^{39}K = 93.1%, ^{40}K = 11.8 ppm, and ^{41}K = 6.0%) (Ref. 10); thus, the contribution of ^{40}K in the analysis was neglected. The ^{41}K contribution to the measured absorption yields lines shifted to the blue by an amount comparable to the hyperfine splitting and is easily included in the line shape analyses.[11]

Discussion of Results

Figure 2 presents representative absorption line shapes recorded from a single laser scan (0.1 ms in duration) during a tunnel run (9.5-MJ/kg total enthalpy) with air as the test gas. The left-hand panel of Fig. 2 is a measured spectrum for the probe beam that propagated at an angle to the flow. Three key absorption features can be seen. The smallest amplitude feature (near 0.68 cm^{-1}) is due to absorption by nearly stationary hot gas adjoining the wall in the probe window boundary layer. The larger amplitude feature has been shown (by numerical solutions of the boundary-layer equations along with equilibrium chemistry calculations) to include the combined absorption of cold freestream potassium and that of relatively hot potassium atoms in the outer portion of the boundary layer, that is, the thermal recovery zone. This combined absorption results in an asymmetric overall line shape for the large absorption feature, with greater width on the right of the peak (labeled freestream absorption) than on the left. Although the length scales in the boundary layer are small compared to the total absorption path length, the concentrations present due to the elevated temperature can be much larger than the freestream. The velocity is determined from the distinct freestream absorption peak present in each laser sweep, as this narrow peak is associated with the potassium in the fast moving freestream.

The right panel of Fig. 2 shows a typical absorbance line shape for the beam propagated orthogonally to the bulk gas velocity. Note that the location of the peak absorbance agrees well with that of the right-hand peak in the left panel of Fig. 2. The measured Doppler shift for this spectral scan corresponds to a freestream velocity of 4.45 km/s, which is in relatively good agreement with the calculated (steady-state) value of 4.16 km/s determined from Calspan computations. The measurement uncertainty in velocity is ±200 m/s, due predominantly to boundary layer absorption.

Figure 3 presents measurements of the temporal variations of gas velocity during a test with a total enthalpy of 9.53 MJ/kg and a freestream temperature of 485 K. The total pressure measurements were recorded at a 100-kHz rate using a nearby pitot probe. Both

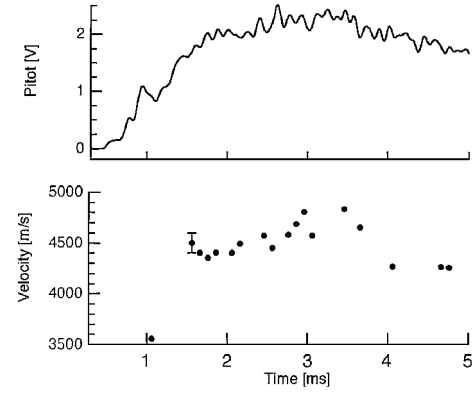

Fig. 3 Measurements of the facility pressure (recorded using a pitot probe) and velocity (recorded using the diode-laser sensor) during a 9.53-MJ/kg test.

ordinate axes share the same abscissa. Note that a period of nearly constant pressure and velocity is observed over a period of about 1.9 ms (from $t = 1.7$ to 3.6 ms in Fig. 3).

The freestream concentration cannot be determined directly, because of the influence of boundary-layer absorption, but an approximate analysis based on a simple model for the boundary layer yields an estimate of 100 parts per billion (freestream).

Conclusion

The characterization of steady-flow test time in hypersonic facilities is often based on pressure or electron number density measurements using pitot probes or microwave interferometry, respectively. The diode-laser measurements of velocity provide an independent and complementary means of determining this flow characteristic in hypersonic test facilities. In addition, diode-laser absorption measurements may also be used to determine the temperature in the test gas from the measured Doppler-broadened line shape or from the ratio of measured absorption lines and species concentrations from the measured absorbance and the gas temperature.[6,7]

This unique and relatively simple and economical probe demonstrated that trace quantities of potassium atoms, naturally present in reflected shock tunnels, can be used to measure velocity. Probes of this type should prove useful for measurements in both small-scale and large-scale facilities. For example, the sensor could be located near a test model for measurements in large-scale hypersonic test facilities. Currently, the probe is being modified to include transpiration cooling to ameliorate the masking of the freestream absorption by the hot boundary-layer gas, and techniques for seeding controlled low levels of potassium into the shock tube are being evaluated. The new probe will subsequently be utilized for velocity measurements in hypersonic flow generated in the Stanford expansion tube.

Acknowledgments

This research was supported by the U.S. Air Force Office of Scientific Research, Aerospace Sciences and Materials Directorate, with Julian Tishkoff as Technical Monitor. The authors gratefully acknowledge the assistance of Kenneth Chadwick and the crew at Calspan Corporation.

References

[1]Wittliff, C. E., Wilson, M. R., and Hertzberg, A., "The Tailored-Interface Hypersonic Shock Tunnel," *Journal of the Aerospace Sciences*, Vol. 26, No. 4, 1959, pp. 219–228.

[2]Lordi, J. A., Mates, R. E., and Moselle, J. R., "Computer Program for the Numerical Solution of Nonequilibrium Expansions of Reacting Gas Mixtures," NASA CR-472, May 1979.

[3]Chadwick, K. M., Holden, M. S., Korte, J. J., and Anderson, E. C., "Design and Fabrication of a Mach 8 Contoured Nozzle for the LENS Facility," AIAA Paper 96-0585, Jan. 1996.

[4]Albrechcinski, T. A., Boyer, D. W., Chadwick, K. M., and Lordi, J. A., "Calspan's Upgraded 96" Hypersonic Shock Tunnel: Its Development and Application in the Performance of Research and Testing at Higher Enthalpies," AIAA Paper 95-0236, Jan. 1995.

[5]Hanson, R. K., "Advanced Laser-Based Diagnostics for Shock Tube/Tunnel Flows," *Proceedings of the 21st International Symposium on Shock Waves*, edited by A. F. P. Houwing, Panther Publishing, Fyshwick, ACT, Australia, 1997, pp. 27–32.

[6]Wehe, S. D., Baer, D. S., and Hanson, R. K., "Tunable Diode-Laser Absorption Measurements of Temperature, Velocity, and H_2O in Hypervelocity Flows," AIAA Paper 97-3267, July 1997.

[7]Baer, D. S., Nagali, V., Furlong, E. R., and Hanson, R. K., "Scanned- and Fixed-Wavelength Absorption Diagnostics for Combustion Measurements Using Multiplexed Diode Lasers," *AIAA Journal*, Vol. 34, No. 3, 1996, pp. 489–493.

[8]Alkemade, C. T. J., *Metal Vapours in Flames*, Pergamon, Oxford, 1982, Chap. 3.

[9]Volz, U., and Schmoranzer, H., "Precision Lifetime Measurements on Alkali Atoms and on Helium by Beam-Gas-Laser Spectroscopy," *Physica Scripta*, Vol. T65, 1996, pp. 48–56.

[10]Lide, D. R., *CRC Handbook of Chemistry and Physics No. 78*, CRC Press, Boca Raton, FL, 1997, p. 10.

[11]Radzig, A. A., and Smirnov, B. M., *Reference Data on Atoms Molecules and Ions*, Vol. 31, Springer–Verlag Series in Chemical Physics, Springer–Verlag, New York, 1985, p. 112.

R. P. Lucht
Associate Editor

UV Raman and Fluorescence Flame Spectroscopy Using a Sheridon Grating Spectrograph

Joseph A. Wehrmeyer*
Vanderbilt University, Nashville, Tennessee 37235

Introduction

ULTRAVIOLET (UV) Raman and predissociative fluorescence spectroscopy have become well-established techniques for obtaining major and minor species concentration and temperature measurements in flames.[1] Advantages of UV over visible excitation include increased scattering cross sections and high laser pulse energy. However, experimental complexity is also increased, especially with respect to optical filtering. Interference bandpass filters, centered around a particular Raman wavelength, have been used successfully for two-dimensional visible Raman imaging of a single molecular species,[2,3] but such filters degrade in performance moving from visible to UV wavelengths. Typical UV interference bandpass filter specifications include passband transmittances of 20% for bandwidths of 26 nm, with transmittance dropping to 12% for 12-nm bandwidths.[4] As a result, a spectrometer is used almost exclusively with UV Raman to provide spectral separation while still offering adequate detection efficiency. An additional benefit of the spectrometer is that it offers the capability of simultaneously measuring the Raman signals from several molecular species.

Received 20 November 1998; revision received 8 March 1999; accepted for publication 5 April 1999.

*Research Associate Professor, Department of Mechanical Engineering, Box 1592 Station B. Senior Member AIAA.

By the use of spectrometers, instantaneous multispecies UV Raman measurements, containing one dimensionally resolved (linewise) spatial information, have been demonstrated.[5,6] The linewise UV Raman technique, using the 248-nm KrF excimer laser, has been extensively used to probe diluted,[7] swirled,[8] or lifted[9] hydrogen jet diffusion flames and has even been used in investigations of an oil-fired furnace burner,[10] an optically accessible spark ignition engine,[10] and an optically accessible rocket engine.[11] In general these research efforts use some form of filtering to reduce the intensity of Rayleigh and Mie scattered light entering the spectrometer, and hence, stray light interference with the relatively weak Raman signals is reduced. Such filtering consists of either a liquid butyl acetate filter,[5,10,11] with a 10-mm path length providing about three orders of magnitude attenuation at 248 nm, or one or more interference negative-bandpass (notch) filters,[9,10] each one attenuating the Rayleigh and Mie scattering by approximately two orders of magnitude. Both the liquid and notch filters attenuate the Raman signals lying close in wavelength to the Rayleigh line, i.e., the O_2 and CO_2 vibrational Q branches and the H_2 rotational O and S branches. The liquid filter also absorbs all wavelengths shorter than 248 nm, which includes the Raman anti-Stokes signals.

If the stray light performance of the imaging spectrograph used in a UV Raman system were improved, then less filtering would be required, thereby allowing better detection efficiency at wavelengths close to the Rayleigh wavelength and even allowing anti-Stokes wavelength detection for systems where butyl acetate filters would no longer be required. One way to improve the stray light performance of a spectrograph is to use holographically ruled gratings. Overall stray light of a holographic grating is up to a factor of 10 less than for a mechanically ruled grating and has no preferred direction; it radiates diffusely through 2π sr, rather than being higher near the diffraction orders as for mechanically ruled gratings.[12,13] However, holographically ruled gratings have relatively poor diffraction efficiency, especially in the UV, compared to mechanically ruled gratings. By ion etching a holographically ruled grating's curved grooves into triangular grooves, efficiency is greatly improved, but the etching process roughens the grooves' surface, thereby degrading stray light performance. In general all of the previous UV Raman investigations have used either mechanically ruled or ion-etched holographically ruled gratings, but there exists an attractive grating alternative.

Holographically ruled gratings can receive near-triangular groove shapes without ion etching through the Sheridon recording method.[13,14] Thus high efficiency and low stray light are simultaneously obtained in a Sheridon holographically ruled grating. These gratings are not widespread because the typical visible wavelengths used in their creation, coupled with the index of refraction of the photoresist used to create the grooves, limits the optimum efficiency wavelength, or blaze wavelength, to a maximum of 250 nm. Yet for 248-nm KrF excimer laser spectroscopy this is an ideal blaze wavelength. This Technical Note shows an experimental comparison, using UV Raman and fluorescence spectroscopy, between a mechanically ruled and a Sheridon holographically ruled grating to demonstrate the superior stray light performance of the latter grating type.

Experimental

The multispecies, linewise Raman/fluorescence images shown in Fig. 1 are obtained from a slightly lean, propane–O_2 flame produced over a Hencken burner. The output from a Lambda–Physik COMPex 150T narrowband, tunable KrF excimer laser is focused into the flame using a 2-m focal length lens, producing a beam waist of ~1 mm diameter. The laser is tuned to 248.395 nm to minimize the production of either OH or O_2 fluorescence.[15,16] Several O_2 and OH transitions are within the tuning range of the KrF laser, and 248.395 nm does not fall directly on any of these transitions. However, about 5% of the laser's output ranges from 248 to 249 nm, resulting in broadband O_2 or OH excitation and subsequent fluorescence.

Raman and Rayleigh scattering are collected at right angles to the laser beam using a 50-mm-diam, 250-mm-focal-length ($f/5$) fused silica air-spaced doublet, and a second identical lens set focuses the